ChemPubSoc Europe

DOI: 10.1002/chem.201500270

CHEMISTRY A European Journal Full Paper

Organocatalysis |*Hot Paper*|

Aromatic Interactions in Organocatalyst Design: Augmenting Selectivity Reversal in Iminium Ion Activation

Mareike C. Holland,[a, b] Jan Benedikt Metternich,[a] Constantin Daniliuc,[a] W. Bernd Schweizer,[c] and Ryan Gilmour*[a, d]

Dedicated to Prof. Dr. Günter Haufe on the occasion of his 65th birthday

Abstract: Substituting *N*-methylpyrrole for *N*-methyindole in secondary-amine-catalysed Friedel–Crafts reactions leads to a curious erosion of enantioselectivity. In extreme cases, this substrate dependence can lead to an inversion in the sense of enantioinduction. Indeed, these closely similar transformations require two structurally distinct catalysts to obtain comparable selectivities. Herein a focussed molecular editing study is disclosed to illuminate the structural features responsible for this disparity, and thus identify lead catalyst structures to further exploit this selectivity reversal. Key to effective catalyst re-engineering was delineating the non-covalent interactions that manifest themselves in conformation. Herein we disclose preliminary validation that intermolecular aromatic (CH–π and cation–π) interactions between the incipient iminium cation and the indole ring system is key to rationalising selectivity reversal. This is absent in the *N*-methylpyrrole alkylation, thus forming the basis of two competing enantio-induction pathways. A simple L-valine catalyst has been developed that significantly augments this interaction.

Introduction

Organocatalysis intermediates are excellent platforms from which to study the non-covalent interactions that control biomolecular structure and function.[1,2] This is particularly true for the α,β-unsaturated iminium salts derived from the MacMillan imidazolidinones (e.g. **1** + **2**→**3**; Figure 1).[3] Unsurprisingly, the conformational behaviour of these phenylalanine derivatives is governed by intramolecular CH–π and π–π interactions; these are pervasive in larger proteins that are rich in aromatic amino acid side chains.[4] Consequently, investigating the role of non-covalent interactions in controlling the conformation and reactivity of iminium ion intermediates has become a vibrant aspect of covalent organocatalysis.[1,5–7] The enantioselective Friedel–Crafts alkylation of *N*-methylpyrrole developed by MacMillan and co-workers[8] has emerged as a valuable catalysis manifold for such investigations.[9,10] This system is well behaved, with intentionally disruptive structural changes mani-

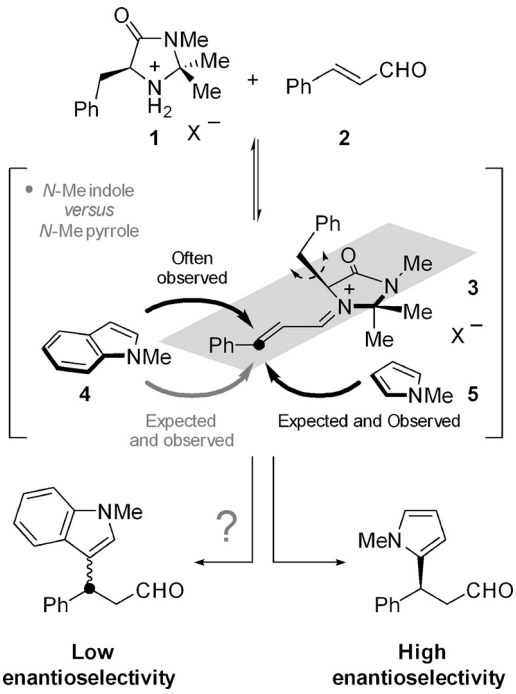

Figure 1. The organocatalytic Friedel–Crafts reactions of *N*-methylindole **4** (left) and *N*-methylpyrrole **5** (right).

[a] *Dr. M. C. Holland,[+] J. B. Metternich,[+] Dr. C. Daniliuc, Prof. Dr. R. Gilmour*
Institut für Organische Chemie
Westfälische Wilhelms-Universität Münster
Corrensstrasse 40, 48149 Münster (Germany)
E-mail: ryan.gilmour@uni-muenster.de
Homepage: http://www.uni-muenster.de/Chemie.oc/gilmour/

[b] *Dr. M. C. Holland[+]*
Current address: Department of Chemistry and Biochemistry
University of California Los Angeles
607 Charles E. Young Drive East, Los Angeles 90095-1569 (USA)

[c] *Dr. W. B. Schweizer*
Laboratorium für Organische Chemie, ETH Zürich
Vladimir-Prelog-Weg 3, 8093 Zürich (Switzerland)

[d] *Prof. Dr. R. Gilmour*
*Excellence Cluster EXC 1003 "*Cells in Motion*"*
Westfälische Wilhelms-Universität Münster, Münster (Germany)

[+] *Both authors contributed equally to this work.*

Supporting information for this article is available on the WWW under http://dx.doi.org/10.1002/chem.201500270.

festing themselves in decreased enantioselectivities. However, studies from this laboratory, and also from Seebach and Grošelj, have revealed that switching from *N*-methylpyrrole (**5**) to *N*-methylindole (**4**)[11,12] causes a severe erosion of the enantioselectivity.[13] Often even modest structural modifications to the catalyst can result in an inversion in the sense of enantio-induction (Figure 1).[14] Motivated by this intriguing selectivity disparity, and the likely interplay of directing non-covalent interactions in catalysis, a molecular editing study of catalyst **1** was initiated to 1) delineate the structural features responsible for this unprecedented induction mode, and 2) generalise the phenomenon.

Whilst studying intermolecular interactions in the reactive iminium ion intermediate **3** by classical spectroscopic and crystallographic techniques[15] is now well established in mechanistic organocatalysis, the study of intermolecular interactions between the iminium ion and substrate remains challenging.[16] Nonetheless, it seems reasonable that such a scenario may be operational in this case.

Just as the *syn*-methyl group of the imidazolidinone core can interact with the proximal phenyl ring in a stabilising, intramolecular CH–π interaction (Figure 2; upper right),[10a,15] it is conceivable that an analogous, intermolecular interaction might occur with highly electron rich Friedel–Crafts substrates such as *N*-methylindole (Figure 2).[17] Such an intermolecular interaction (Path I) may then give rise to a directing effect which competes with conventional steric induction (Path II).[18] This phenomenon would manifest itself in severely diminished enantioselectivity, and in some cases invert the inherent sense of enantio-induction. The differing steric and electronic signatures of the side-arm benzyl ring (intramolecular interaction), *N*-methylpyrrole and *N*-methylindole (intermolecular interactions) may be a clue to this phenomenon. Consequently, the traceless quadrupole moment tensors orthogonal to the aryl ring (Q_{zz}) were calculated, revealing that for *N*-methylpyrrole $Q_{zz}=-4.10$, *N*-methylindole $Q_{zz}=-4.94$ (5-membered ring) and -5.10 (6-membered ring) (Figure 2, lower).

Further evidence implicating the six-membered ring of *N*-methylindole as being key to this selectivity difference can be gleaned from structural biology and computational studies. Aromatic interactions involving the indole-containing amino acid tryptophan are known to be crucial in controlling protein structure.[19] Computational analyses by Macias and MacKerell have concluded that CH–π interactions to the six-membered ring of tryptophan are stronger than to all other aromatic amino acid side chains.[19d] Furthermore, a computational study of methane–indole complexes by Sherrill and co-workers demonstrated that interactions with the six-membered ring of tryptophan are favoured over those with the five-membered ring.[20] Together with the quadrupole moment differences, these observations make a compelling argument for the importance of an aromatic interaction to rationalise the selectivity variation in switching from *N*-methylpyrrole to *N*-methylindole. Consequently, an aromatic directing model can be envisaged to account for the addition of the nucleophile to the more sterically congested face of the transient iminium π-system.[21] Whilst the concepts of electronic versus sterically controlled selection is well established in secondary amine catalysis,[22] it is traditionally associated with hydrogen-bonding ensembles, in contrast to this postulate.[23]

To validate this notion, a focussed molecular editing study was performed[24] to identify the structural features that influence enantioselection in the alkylation of *N*-methylindole (Figure 3). Specifically, the side-chain region of the corresponding amino acids (R^1) and the aminal substituents (R^2 and R^3) were modified to subtly disrupt the (intramolecular) aromatic interaction that is important in orchestrating induction in the *N*-methylpyrrole alkylation.[21] This intuitive observation stems from the highly delocalised nature of the iminium cation,[25] and the well-described preference of the pendant phenyl ring to align proximal to the *syn*-methyl group of the first-generation catalyst ($R^1=R^2=Me$). Since the Friedel–Crafts alkylation

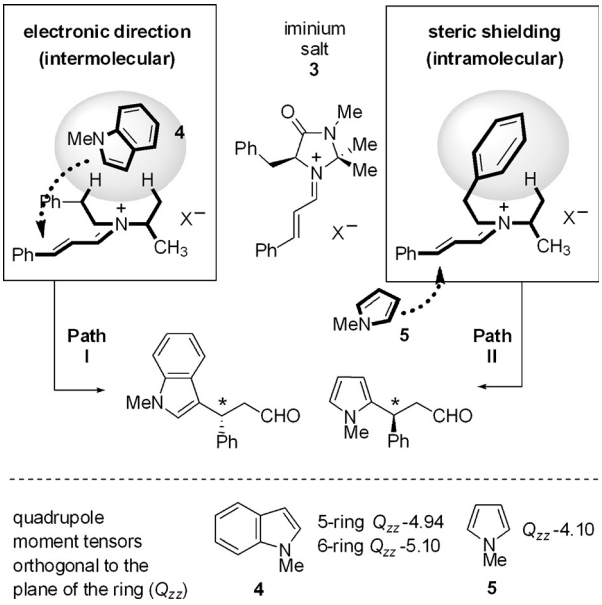

Figure 2. Upper: A directing model to account for the lower enantioselectivity and/or reversal of selectivity in the organocatalytic Friedel–Crafts alkylation of *N*-methylindole (Path I) versus *N*-methylpyrrole (Path II). Lower: The traceless quadrupole moment tensor (Q_{zz}) of *N*-methylindole (**4**) and *N*-methylpyrrole (**5**). Q_{zz} calculated using DFT (TPSS/def2-TZVP).

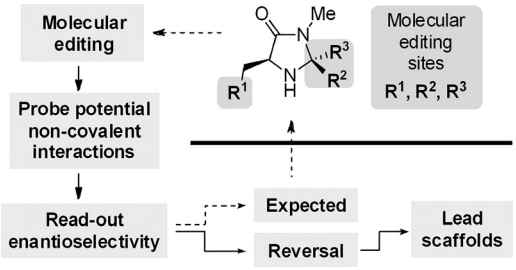

Figure 3. Molecular editing of the MacMillan first-generation catalyst to identify the structural features responsible for selectivity reversal in the Friedel–Crafts alkylation of *N*-methylindole.

of *N*-methylpyrrole catalysed by the first-generation MacMillan catalyst does not display this reverse selectivity tendency, this transformation was performed in parallel with the *N*-methylindole alkylations as a control.

Results and Discussion

Since non-covalent interactions manifest themselves in conformation, systematic variation of positions R^1, R^2 and R^3 was performed to disrupt the optimised geometry of the core first-generation structure (Figure 4). Moreover, the strategic use of

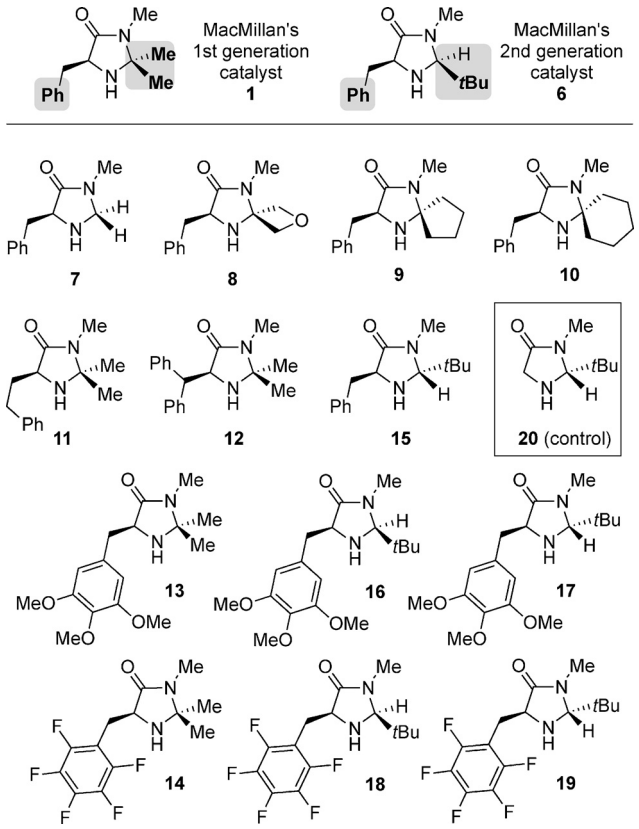

Figure 4. The catalyst library (**1** and **6**–**20**) investigated in the organocatalytic Friedel–Crafts alkylation of *N*-methylindole (**4**) and *N*-methylpyrrole (**5**).

Table 1. Application of catalysts **1** and **6**–**20** in the enantioselective Friedel–Crafts alkylation of *N*-methylpyrrole (**5**) and *N*-methylindole (**4**).[a]

	R^1	Q_{zz}	R^2	R^3	e.r.[b] pyrrole **5**	e.r.[b] indole **4**
1	Ph	−3.46	CH_3	CH_3	92:8	65:35
2	Ph	−3.46	H	H	60:40	54:46
3	Ph	−3.46			61:39	56.5:43.5
4	Ph	−3.46			86:14	67:33
5	Ph	−3.46			67.5:32.5	62:38
6		−3.46	CH_3	CH_3	69:31	36.5:63.5[c]
7		−3.46	CH_3	CH_3	75.5:24.5	60.5:39.5
8		−5.68	CH_3	CH_3	97:3	73:27
9		+3.01	CH_3	CH_3	83:17	40:60[c]
10	Ph	−3.46	*t*Bu	H	92.5:7.5	88:12
11	Ph	−3.46	H	*t*Bu	54:46	50:50
12		−5.68	*t*Bu	H	92:8	77:23
13		−5.68	H	*t*Bu	68:32	58:42
14		+3.01	*t*Bu	H	77:23	84:16
15		+3.01	H	*t*Bu	67:33	45:55
16	glycine	N/A[d]	H	*t*Bu	33:67	23.5:76.5

[a] Full experimental details are provided in the Supporting Information. [b] The product aldehydes were reduced in situ and the enantiomeric ratios were determined for the corresponding alcohols. [c] Selectivity reversal observed. [d] N/A = not applicable.

pentafluorophenyl and trimethoxybenzene rings ($Q_{zz} = +3.01$ and −5.68, respectively) was employed to further delineate the role of the shielding group and probe for the involvement of a cation–π interaction (Table 1).[9c,21]

Initially, a series of imidazolidinone organocatalysts (**1** and **6**–**20**) were prepared which differ in sites R^1, R^2 and R^3 (Figure 4). A number of these catalysts are commercially available or their syntheses have been described elsewhere.[9c,26] Full details are provided in the Supporting Information.

Targets **7**–**14** were conceived based on the first-generation catalyst structure. Catalysts **7**–**10** were designed to distort the position of the key hydrogen atom implicated in the stabilising cation-.π interaction,[9c,10a,21] whilst retaining its proximity to the aryl ring. Since the *syn*-methyl group plays a pivotal role in catalysis, a logical control structure was that with the entire *geminal*-dimethyl moiety deleted (**7**). Re-introducing this feature in the form of a spiro compound (4-, 5- and 6-membered rings, **8**–**10**, respectively) would allow the effect of subtle changes in geometry to be probed: should this interaction be important in catalysis then any disruption would likely manifest itself in decreased selectivity. Similarly, by homologating the arm of the shielding group (**11**), the system would no longer benefit from the characteristic pre-organised geometry of the parent iminium salt (Figure 2). It was envisaged that the (diphenyl)methyl moiety of catalyst **12** might simultaneously interact with the *syn*-methyl group and the pendant iminium chain, thus satisfying both cation–π sites.[9c,21,25] Recently, we have established that electronic modulation of the aryl shielding group has profound effects on the conformation and reactivity of the first-generation iminium salts.[9c] Consequently,

compounds **13** and **14** would serve as electronic extremes of the parent catalyst (**13** $Q_{zz}<0$ and **14** $Q_{zz}>0$). Finally, this process was repeated for the second- generation catalyst furnishing the diastereomer pairs **6**/**15**, and for the electronically modulated systems **16**/**17**, and **18**/**19**. Finally, the gylcine derivate **20** was prepared as a control catalyst.

Collectively, it was envisaged that this library of electronically modulated, homologated, truncated or rigidified analogues would effectively probe the spacial and electronic factors that underpin this tentative induction model. Gratifyingly, a number of these catalyst salts were crystalline (**9**, **10**, **13**, **14** and **18**) and could be characterised by single-crystal X-ray analysis (Figure 5).[27]

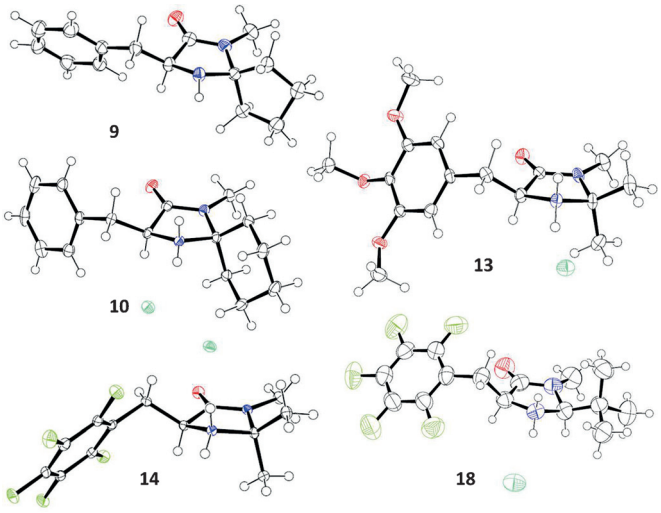

Figure 5. X-ray crystallographic analysis of catalysts **9**, **10**, **13**, **14** and **18**. Thermal ellipsoids shown at the 50% probability level.[27]

In the Friedel–Crafts alkylation of *N*-methylpyrrole with *trans*-cinnamaldehyde catalysed by the first-generation analogues (Figure 1), the parent catalyst (R^1 = Ph,[8] Table 1, entry 1) gave encouraging levels of enantioselectivity at ambient temperature (e.r. 92:8).

Complete deletion of the *gem*-dimethyl motif (entry 2, R^2 = R^3 = H) resulted in a dramatic reduction in selectivity (e.r. 60:40). This may be attributed to the removal of a key structural feature required for the cation–π interaction, but is more likely a consequence of the alleviation of $A^{1,3}$-strain in the incipient iminium ion leading to an geometric (*E*/*Z*) mixture in which both faces are accessible to the nucleophile.[9a]

Substituting the *gem*-dimethyl group by cyclic systems installed flanking C–H units to engage in a cation–π interaction, but introduced geometric constraints including restricted torsional rotation ($\varphi_{H\text{-}C\text{-}C\text{-}N}$), and contracted C-C-C bond angles (Table 1, entries 3–5). The highest levels of enantioselectivity were found with the cyclopentane derivative **9** [(oxetane (e.r. 61:39), cyclopentane (e.r. 86:14), cyclohexane (e.r. 67.5:32.5)]. One carbon homologation of the shielding group proved to be detrimental to selectivity (e.r. 69:31, entry 6) as did installing a diphenylmethyl substitutent (e.r. 75.5:24.5, entry 7). Electronic modulation augmented the enantioselectivity considerably with the more electron-rich trimethoxybenzene derivative (entry 8, $Q_{zz}=-5.68$) delivering the product with the highest enantioselectivities of the study (e.r. 97:3).[9c,21] In contrast, the electron-deficient pentafluorophenyl analogue ($Q_{zz}=+3.01$) gave a notably lower selectivity (entry 9, e.r. 83:17). This observation is consistent with the notion that cation–π interactions are enhanced in electron-rich systems ($Q_{zz}<0$, Figure 6). Consequently, the pentafluorophenyl group has found widespread application as a mechanistic tool to assist in exposing interactions of this type in biological settings.[28]

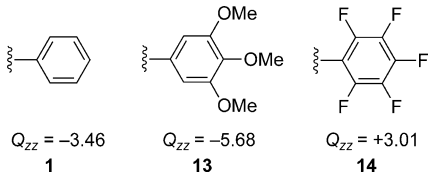

Figure 6. The components of the traceless quadrupole moment tensor orthogonal to the aromatic ring (Debeye-Ångstrom, Q_{zz}) are given for the corresponding toluene derivatives of **1**, **13** and **14**.[9c] Q_{zz} calculated using DFT (TPSS/def2-TZVP).

Analysis of second-generation MacMillan imidazolidinone scaffolds also proved instructive (Table 1, entries 10–16). A simple inversion of the aminal stereocentre caused a dramatic loss of selectivity (e.r. 92.5:7.5→54:46, entries 10 and 11 respectively). Finally, to examine the effect of the electronic changes to R^1 on catalysis, both diastereomers of the trimethoxyphenyl and pentafluorophenyl catalysts were investigated (**16** and **17**, **18** and **19**, entries 12–15). Again, the configuration of the aminal centre was the prevailing factor in conferring induction, with the *syn* derivatives furnishing the highest levels of enantioselectivity (e.r. 92:8 versus 68:32, entries 12 and 13; e.r. 77:23 versus 67:33, entries 14 and 15). The reactions also showed a clear dependence on the electronic nature of the aryl ring, with the trimethoxyphenyl system outperforming the pentafluorophenyl (e.r. 92:8 versus 77:23, entries 12 and 14). In the control experiment with the glycine derived catalyst **20** (entry 16), in which the only source of chiral information in the aminal centre, comparable selectivity was observed as for **19** (entry 15). This suggests that the pentafluorophenyl substituent is not essential for enantioselective catalysis. This observation also provides additional support to an earlier conclusion that the corresponding fluorinated iminium salt has a varied conformational behaviour often populating the conformer in which the aryl ring is distal from the core (C_{ipso}-C-C-N^+ ca. 180°).[9c]

Many of these general trends were observed in the analogous reactions with *N*-methylindole. Deletion or replacement of the *gem*-dimethyl group was detrimental to selectivity (Table 1, entries 2–5), although slightly improved levels of induction were noted with the cyclopentane system (entry 4, e.r. 67:33 versus 65.5:34.5): this is consistent with the *N*-methylpyrrole alkylation. Homologating the side chain by one methylene unit led to an intriguing reversal in the sense of enantioselectivity compared to the first-generation catalyst (e.r. 36.5:63.5

versus 65.5:34.5, entries 6 and 1, respectively). This is diminished in iminium salts derived from catalyst **1**, where the intramolecular interaction dominates. The addition of a second aryl ring in the form of a (diphenyl)methyl unit proved ineffective (entry 7, e.r. 60.5:39.5). Consistent with the *N*-methylpyrrole study, electronic modulation of the aryl shielding group gave significantly different catalysis outcomes. The trimethoxyphenyl derivative outperformed the first-generation catalyst (entry 8), whilst the pentafluorophenyl analogue led to the second selectivity reversal hit (e.r. 40:60, entry 9). Again, this may be a consequence of the decreased tendency of the electron deficient aryl ring to participate in an intramolecular interaction, thus placing the benzylic protons above the catalyst core. A study of the second-generation imidazolidinone scaffold (entries 10–16) once more confirmed the aminal configuration-dependence of selectivity in both transformations (e.r. 88:12 and 50:50, entries 10 and 11 respectively). This was a predominant factor in catalysts irrespective of the electron rich nature of the shielding group (entries 12/13 and 14/15). Consistent with the *N*-methylpyrrole results, the *syn*-diastereomers furnished higher levels of enantioselectivity than the corresponding *anti* systems. However, the pentafluorophenyl catalyst delivered selectivities that approach those of the MacMillan second-generation catalyst. Importantly, complete deletion of the benzyl substituent was remarkably well tolerated (e.r. 23.5:76.5, entry 16).

Having identified catalysts **11** and **14** as lead structures in inverting the intrinsic sense of enantioinduction in organocatalytic Friedel–Crafts alkylation of *N*-methylindole (e.r. 36.5:63.5 and 40:60, respectively), a second iteration of molecular editing was performed (Table 2). Common to both structures is the likely participation of the C2 C-H group (*H*-C-C-N$^+$) in directing the *N*-methylindole to the upper face of the π system either as a consequence of homologation (**11**) or conformation (**14**). In an attempt to augment the tentative aromatic interactions between the catalyst core and the substrate that forms the basis of the working hypothesis, catalysts **21**, **22** and **23** were conceived (Table 2). It was envisaged that by progressively removing aromaticity (entry 1), and subsequently the steric footprint of the shielding arm (entries 2 and 3), it would be possible to enhance the tentative intermolecular cation–π interaction that pre-organises the ensemble prior to C–C bond formation.

To that end, imidazolidinones **21**, **22** and **23** were prepared from the constituent amino acids: gratifyingly the structures of compounds **21** and **23** could be unequivocally established by X-ray crystallography (Figure 7). The three catalysts were independently exposed to *trans*-cinnamaldehyde and *N*-methylindole at ambient temperature (Table 2). The analogous reactions with *N*-methylpyrrole were performed in parallel as a control. As expected, catalyst **21**–**23** proved to be perfectly competent catalysts in the alkylation of *N*-methylpyrrole, albeit with modest levels of enantiocontrol (up to e.r. 69:31).

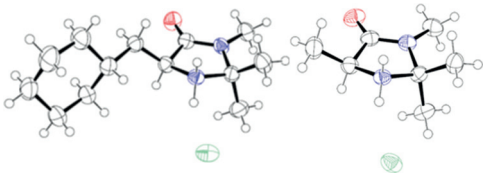

Figure 7. X-ray crystal structure analysis of catalysts **21** (HCl salt) and **23** (HCl salt). Thermal ellipsoids shown at the 50% probability level.[28]

However, switching to *N*-methylindole resulted in a general inversion of the sense of enantiocontrol. This was most pronounced with the L-valine derivative **22** for which an enantiomeric ratio of 25:75 was obtained. Remarkably, this could be enhanced to 14.5:85.5 at −55 °C.

The comparative analysis of *N*-methylpyrrole and *N*-methylindole in Friedel–Crafts alkylations is consistent with the notion that two distinct induction pathways are operational, (Figure 2). This difference may be rationalised by invoking aromatic interactions between the substrate and the more sterically congested face of the electrophile. Consequently, the C2 and C5 substituents of the imidazolidinone core pre-organise the electron-rich *N*-methylindole prior to addition, thus forming the basis of an induction model. Moreover, this would also serve to increase the proximity of the reactants; a quintessential feature of enzyme catalysis.

Compelling experimental evidence suggests that the area above the catalyst core is key to understanding this selectivity difference (Figure 2). However, the geometrical constraints of this intermolecular interaction are not immediately obvious. Initially, it was assumed that a pincer-type model may be operational, such that several cation/CH–π interactions[9c,10a,21] would operate synergistically to pre-organise the ensemble. However, this would necessarily position the two π systems orthogonal to each other, thus introduce orbital constraints which would require a process of realignment prior to productive bond formation. Alternatively, a "sticky surface" model can be envisaged in which multiple the C–H bonds can interact with the same face of the electron-rich heterocycle.

Table 2. Application of catalysts **21**, **22** and **23** in the enantioselective Friedel–Crafts alkylation of *N*-methylpyrrole and *N*-methylindole.[a]

	Catalyst	e.r.[b] *N*-Me pyrrole **5**	e.r.[b] *N*-Me indole **4**
1	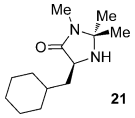 **21**	69:31	39:61[c]
2	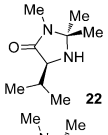 **22**	63:37	25:75[c] 14.5:85.5[d]
3	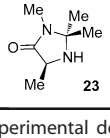 **23**	63.5:36.5	33:67[c]

[a] Full experimental details are provided in the Supporting Information. [b] The product aldehydes were reduced in situ and the enantioselectivities were determined for the corresponding alcohols. [c] Selectivity reversal observed. [d] Reaction performed at −55 °C.

In an attempt to probe the interaction of the iminium ion with the *N*-methylindole, the tryptophan derived imidazolidinone **24** and the corresponding iminium salt **25** were prepared and characterised by single-crystal X-ray diffraction (Figure 8).[30] Immediately evident from this analysis was that

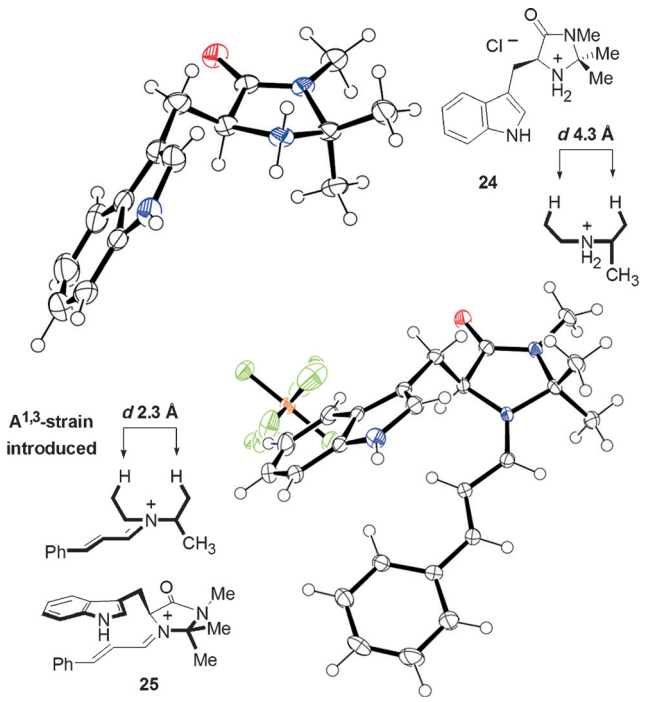

Figure 8. X-ray crystal structure analysis of catalysts **24** (HCl salt) and **25** ($HSbF_6$ salt). Thermal ellipsoids shown at the 50% probability level.[30] In the upper structure the chloride anion has been omitted for clarity. Note that the increased $A^{1,3}$-strain in the iminium salt **25** results in a significant shortening of the distance between the C–H bonds (2.3 versus 4.3 Å).

formation of the iminium ion induces a compression of the C2 and C5 substituents above the catalyst core; this general phenomenon in imidazolidinone-derived iminium ions is a consequence of increased $A^{1,3}$-strain. Consequently, the distance of the neighbouring C–H moieties at the C2 and C5 positions contracts from 4.3 to 2.4 Å. This would preclude formation of a pincer-type complex with orthogonal π systems. Accordingly, it is conceivable that the *N*-methylindole interacts with the iminium cation through both rings by means of a "sticky surface" mode; this is in accordance with Sherrill and co-workers theoretical study of methane–indole complexes, although the nature of the interaction in this scenario requires clarification (Figure 9).[20] Solution-phase conformational analysis of the L-valine-derived iminium salt **26** revealed key nOe contacts that are consistent with one of the methyl groups of the isopropyl substituent residing in the *synclinal-endo* conformation. This is fully consistent with the Sherril model (for full details see the Supporting Information). This conformation has also been observed in a structurally related L-valine-derived auxiliary by Seebach and co-workers.[31] Subsequent slippage of the *N*-methylindole onto the iminium π system, conceivably bearing some resemblance to the X-ray structure of **25**, would then satisfy the stereoelectronic requirements for bond formation and account for this intriguing reversal of selectivity (Figure 9).

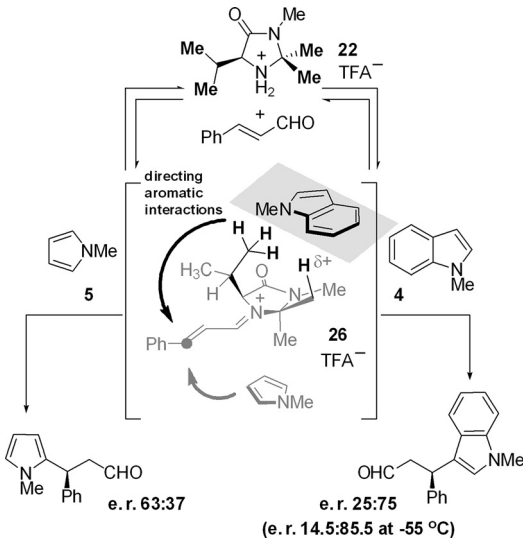

Figure 9. A simple L-valine derived catalyst (**22**) alters the sense of enantioinduction.

It is also interesting to note that the X-ray structure of **25** is a rare example of an iminium salt in which the aryl ring is oriented above the π system.[9]

Conclusion

Herein we disclose experimental validation of a novel directing effect based on multiple aromatic interactions between an imidazolidinone-derived iminium ion and *N*-methylindole.[32] This study suggests that a subtle interplay of CH–π and cation–π interactions between the covalent organocatalysis intermediate (C2 and C5) and substrate not only enhances proximity, but also serves to pre-organise the ensemble prior to reaction. This "sticky surface" concept invoking dispersion interactions likely increases the effective reagent concentration prior to the enantiodetermining C–C bond forming process; this accounts for the contrasting behaviour of *N*-methylindole and *N*-methylpyrrole in organocatalytic Friedel–Crafts alkyations. A focussed molecular editing study was performed to identify the structural features responsible for this disparity. By reverse-engineering the catalyst it has been possible to significantly augment this reversal of selectivity with a valine derivative (e.r. 85.5:14.5, Figure 10). Further application of this and related induction

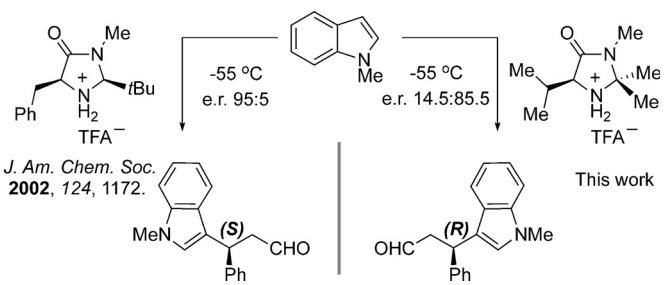

Figure 10. Catalyst re-engineering can lead to an inversion in the sense of enantioselectivity in the Friedel–Crafts alkylation of *N*-methylindole.

modes based on non-covalent interactions[33] are currently ongoing and will be reported in due course.

Experimental Section

Full experimental details are provided in the Supporting Information.

Acknowledgements

This work was generously supported by the WWU Münster, the Deutsche Forschungsgemeinschaft (SFB 858 and Excellence Cluster EXC 1003 "*Cells in Motion—Cluster of Excellence*"). We thank Dr. Christian Mück-Lichtenfeld for calculating the traceless quadrupole moment tensors (Q_{zz}), and Professors Jack D. Dunitz and Dieter Seebach (ETH Zürich) for their interest in this work.

Keywords: CH–π/cation–π interactions · imidazolidinone · molecular design · non-covalent interactions · selectivity reversal

[1] a) M. C. Holland, R. Gilmour, *Angew. Chem. Int. Ed.* **2015**, *54*, 3862 – 3871; *Angew. Chem.* **2015**, *127*, 3934 – 3943; b) R. R. Knowles, E. N. Jacobsen, *Proc. Natl. Acad. Sci. USA* **2010**, *107*, 20678 – 20685.

[2] M. Raynal, P. Ballester, A. Vidal-Ferran, P. W. N. M. van Leeuwen, *Chem. Soc. Rev.* **2014**, *43*, 1660 – 1733.

[3] For selected examples see a) K. A. Ahrendt, C. J. Borths, D. W. C. MacMillan, *J. Am. Chem. Soc.* **2000**, *122*, 4243 – 4244; b) W. S. Jen, J. J. M. Wiener, D. W. C. MacMillan, *J. Am. Chem. Soc.* **2000**, *122*, 9874 – 9875; c) A. B. Northrup, D. W. C. MacMillan, *J. Am. Chem. Soc.* **2002**, *124*, 2458 – 2460; d) N. A. Paras, D. W. C. MacMillan, *J. Am. Chem. Soc.* **2002**, *124*, 7894 – 7895; e) S. P. Brown, N. C. Goodwin, D. W. C. MacMillan, *J. Am. Chem. Soc.* **2003**, *125*, 1192 – 1194; f) J. F. Austin, S. G. Kim, C. J. Sinz, W. J. Xiao, D. W. C. MacMillan, *Proc. Natl. Acad. Sci. USA* **2004**, *101*, 5482 – 5487; g) R. M. Wilson, W. S. Jen, D. W. C. MacMillan, *J. Am. Chem. Soc.* **2005**, *127*, 11616 – 11617; h) Y. Huang, A. M. Walji, C. H. Larsen, D. W. C. MacMillan, *J. Am. Chem. Soc.* **2005**, *127*, 15051 – 15053; i) S. Lee, D. W. C. MacMillan, *Tetrahedron* **2006**, *62*, 11413 – 11424; j) J. B. Tuttle, S. G. Ouellet, D. W. C. MacMillan, *J. Am. Chem. Soc.* **2006**, *128*, 12662 – 12663; k) D. W. C. MacMillan, *Nature* **2008**, *455*, 304 – 308.

[4] a) M. Brandl, M. S. Weiss, A. Jabs, J. Sühnel, R. Hilgenfeld, *J. Mol. Biol.* **2001**, *307*, 357 – 377; b) M. L. Waters, *Curr. Opin. Chem. Biol.* **2002**, *6*, 736 – 741; c) M. J. Plevin, D. L. Bryce, J. Boisbouvier, *Nat. Chem.* **2010**, *2*, 466 – 471.

[5] For selected reviews see a) A. Erkkilä, I. Majander, P. M. Pihko, *Chem. Rev.* **2007**, *107*, 5416 – 5470; b) P. Melchiorre, M. Marigo, A. Carlone, G. Bartoli, *Angew. Chem. Int. Ed.* **2008**, *47*, 6138 – 6171; *Angew. Chem.* **2008**, *120*, 6232 – 6265; c) S. Bertelsen, K. A. Jørgensen, *Chem. Soc. Rev.* **2009**, *38*, 2178 – 2189; d) L. E. Zimmer, C. Sparr, R. Gilmour, *Angew. Chem. Int. Ed.* **2011**, *50*, 11860 – 11871; *Angew. Chem.* **2011**, *123*, 12062 – 12074.

[6] For the example of cyclopropyliminium activation see C. Sparr, R. Gilmour, *Angew. Chem. Int. Ed.* **2011**, *50*, 8391 – 8395; *Angew. Chem.* **2011**, *123*, 8541 – 8545.

[7] a) S. Lakhdar, T. Tokuyasu, H. Mayr, *Angew. Chem. Int. Ed.* **2008**, *47*, 8723 – 8726; *Angew. Chem.* **2008**, *120*, 8851 – 8854; b) G. Evans, T. J. K. Gibbs, R. L. Jenkins, S. J. Coles, M. B. Hursthouse, J. A. Platts, N. C. O. Tomkinson, *Angew. Chem. Int. Ed.* **2008**, *47*, 2820 – 2823; *Angew. Chem.* **2008**, *120*, 2862 – 2865; c) J. B. Brazier, K. M. Jones, J. A. Platts, N. C. O. Tomkinson, *Angew. Chem. Int. Ed.* **2011**, *50*, 1613 – 1616; *Angew. Chem.* **2011**, *123*, 1651 – 1654; d) H. Mayr, S. Lakhdar, B. Maji, A. R. Ofial, *Beilstein J. Org. Chem.* **2012**, *8*, 1458 – 1478; e) Mayr Database: http://www.cup.lmu.de/oc/mayr/reaktionsdatenbank/.

[8] N. A. Paras, D. W. C. MacMillan, *J. Am. Chem. Soc.* **2001**, *123*, 4370 – 4371.

[9] For selected examples see a) C. Sparr, R. Gilmour, *Angew. Chem. Int. Ed.* **2010**, *49*, 6520 – 6523; *Angew. Chem.* **2010**, *122*, 6670 – 6673; b) S. Lakhdar, H. Mayr, *Chem. Commun.* **2011**, *47*, 1866 – 1868; c) M. C. Holland, S. Paul, W. B. Schweizer, K. Bergander, C. Mück-Lichtenfeld, S. Lakhdar, H. Mayr, R. Gilmour, *Angew. Chem. Int. Ed.* **2013**, *52*, 7967 – 7971; *Angew. Chem.* **2013**, *125*, 8125 – 8129.

[10] a) R. Gordillo, J. Carter, K. N. Houk, *Adv. Synth. Catal.* **2004**, *346*, 1175 – 1185; b) for an excellent review see P. H.-Y. Cheong, C. Y. Legault, J. M. Um, N. Çelebi-Ölçüm, K. N. Houk, *Chem. Rev.* **2011**, *111*, 5042 – 5137.

[11] J. F. Austin, D. W. C. MacMillan, *J. Am. Chem. Soc.* **2002**, *124*, 1172 – 1173.

[12] For selected examples of organocatalytic Friedel–Crafts alkylation of indoles see a) G. Bartoli, M. Bosco, A. Carlone, F. Pisciaioli, L. Sambri, P. Melchiorre, *Org. Lett.* **2007**, *9*, 1403 – 1405; b) W. Chen, W. Du, L. Yue, R. Li, Y. Wu, L. S. Ding, Y. C. Chen, *Org. Biomol. Chem.* **2007**, *5*, 816 – 821.

[13] a) C. Sparr, Ph. D. Dissertation 19894, ETH Zürich **2011**; b) U. Grošelj, Č. Podlipnik, J. Bezenšek, J. Svete, B. Stanovnik, D. Seebach, *Helv. Chim. Acta* **2014**, *97*, 1815 – 1821.

[14] M. Bartók, *Chem. Rev.* **2010**, *110*, 1663 – 1705.

[15] For selected structural studies see a) D. Seebach, U. Grošelj, D. M. Badine, W. B. Schweizer, A. K. Beck, *Helv. Chim. Acta* **2008**, *91*, 1999 – 2034; b) J. B. Brazier, G. Evans, T. J. K. Gibbs, S. J. Coles, M. B. Hursthouse, J. A. Platts, N. C. O. Tomkinson, *Org. Lett.* **2009**, *11*, 133 – 136; c) M. C. Holland, G. Berden, J. Oomens, A. J. H. M. Meijer, M. Schäfer, R. Gilmour, *Eur. J. Org. Chem.* **2014**, 5675 – 5680; d) For the X-ray structure of the MacMillan catalyst see J. C. Burley, R. Gilmour, T. J. Prior, G. M. Day, *Acta Crystallogr. Sect. C* **2008**, *64*, o10 – o14.

[16] For beautiful investigations of intermolecular interactions see a) H. Adams, F. J. Carver, C. A. Hunter, J. C. Morales, E. M. Seward, *Angew. Chem. Int. Ed. Engl.* **1996**, *35*, 1542 – 1544; *Angew. Chem.* **1996**, *108*, 1628 – 1631; b) F. J. Carver, C. A. Hunter, E. M. Seward, *Chem. Commun.* **1998**, 775 – 776.

[17] For selected reviews on CH–π interactions see a) M. Nishio, M. Hirota, Y. Umezawa, *The CH/π Interaction: Evidence, Nature and Consequences*, Wiley-VCH, Weinheim, **1998**; b) J. C. Ma, D. A. Dougherty, *Chem. Rev.* **1997**, *97*, 1303 – 1324; c) J. P. Gallivan, D. A. Dougherty, *Proc. Natl. Acad. Sci. USA* **1999**, *96*, 9459 – 9464; d) L. M. Salonen, M. Ellermann, F. Diederich, *Angew. Chem. Int. Ed.* **2011**, *50*, 4808 – 4842; *Angew. Chem.* **2011**, *123*, 4908 – 4944.

[18] D. Seebach, U. Grošelj, W. B. Schweizer, S. Grimme, C. Mück-Lichtenfeld, *Helv. Chim. Acta* **2010**, *93*, 1 – 16.

[19] a) D. A. Dougherty, *J. Nutr.* **2007**, *137*, 1504S – 1508S; b) D. A. Dougherty, *Science* **1996**, *271*, 163 – 168; c) F. N. R. Petersen, M. Ø. Jensen, C. H. Nielsen, *Biophys. J.* **2005**, *89*, 3985 – 3996; d) A. T. Macias, A. D. MacKerell, *J. Comput. Chem.* **2005**, *26*, 1452 – 1463.

[20] A. L. Ringer, M. S. Figgs, M. O. Sinnokrot, C. D. Sherrill, *J. Phys. Chem. A* **2006**, *110*, 10822 – 10828.

[21] This laboratory has recently reported that the intramolecular CH – π interaction may be considered as a cation – π interaction owing to the highly delocalised nature of the iminium cation. The quadrupole moment (Q_{zz}) correlates linearly with enantioselectivity in a range of catalytic transformations. M. C. Holland, J. B. Metternich, C. Mück-Lichtenfeld, R. Gilmour, *Chem. Commun.* **2015**, *51*, 5322 – 5325.

[22] M. Nielsen, D. Worgull, T. Zweifel, B. Gschwend, S. Bertelsen, K. A. Jørgensen, *Chem. Commun.* **2011**, *47*, 632 – 649.

[23] Accounting for the reversal of selectivity by implicating an iminium isomerization–addition sequence seems unlikely based on considerations of 1,3-allylic strain a) R. W. Hoffmann, *Chem. Rev.* **1989**, *89*, 1841 – 1860; b) D. Seebach, B. Amatsch, R. Amstutz, A. K. Beck, M. Doler, M. Egli, R. Fitzi, M. Gautschi, B. Herradön, P. C. Hidber, J. J. Irwin, R. Locher, M. Maestro, T. Maetzke, A. Mouriño, E. Pfammatter, D. A. Plattner, C. Schickli, W. B. Schweizer, P. Seiler, G. Stucky, W. Petter, J. Escalante, E. Juaristi, D. Quintana, C. Miravitlles, E. Molins, *Helv. Chim. Acta* **1992**, *75*, 913 – 934.

[24] E.-M. Tanzer, L. E. Zimmer, W. B. Schweizer, R. Gilmour, *Chem. Eur. J.* **2012**, *18*, 11334 – 11342.

[25] For a computational study of the second-generation MacMillan catalyst see Y. Mori, S. Yamada, *Molecules* **2012**, *17*, 2161 – 2168.

[26] For representative protocols for the synthesis of the MacMillan catalyst and derivatives thereof see a) G. Lelais, D. W. C. MacMillan, *Aldrichimica Acta* **2006**, *39*, 79 – 87; b) D. Seebach, R. Gilmour, U. Grošelj, G. Deniau, C. Sparr, M.-O. Ebert, A. K. Beck, L. B. McCusker, D. Šišak, T. Uchimaru,

Helv. Chim. Acta **2010**, *93*, 603 – 634; c) L. Samulis, N. C. O. Tomkinson, *Tetrahedron* **2011**, *67*, 4263 – 4267; d) T. H. Graham, B. D. Horning, D. W. C. MacMillan, *Org. Synth.* **2011**, *88*, 42 – 53; e) U. Grošelj, A. K. Beck, W. B. Schweizer, D. Seebach, *Helv. Chim. Acta* **2014**, *97*, 751 – 796.

[27] CCDC 1035248 (**9**), 1035249 (**10**), 1035250 (**13**), 1035577 (**14**) and 1035266 (**18**) contain the supplementary crystallographic data for this paper. These data can be obtained free of charge from The Cambridge Crystallographic Data Centre via www.ccdc.cam.ac.uk/data_request/cif.

[28] For an experimental determination of a cation-π interaction in triterpene biosynthesis see: N. Morikubo, Y. Fukuda, K. Ohtake, N. Shinya, D. Kiga, K. Sakamoto, M. Asanuma, H. Hirota, S. Yokoyama, T. Hoshino, *J. Am. Chem. Soc.* **2006**, *128*, 13184 – 13194.

[29] CCDC 1035268 (**21**) and 1035267 (**23**) contain the supplementary crystallographic data for this paper. These data can be obtained free of charge from The Cambridge Crystallographic Data Centre via www.ccdc.cam.ac.uk/data_request/cif.

[30] CCDC 1035253 (**24**) and 1035251 (**25**) contain the supplementary crystallographic data for this paper. These data can be obtained free of charge from The Cambridge Crystallographic Data Centre via www.ccdc.cam.ac.uk/data_request/cif.

[31] C. Gaul, W. B. Schweizer, P. Seiler, D. Seebach, *Helv. Chim. Acta* **2002**, *85*, 1546 – 1566.

[32] For beautiful examples of the strategic use of aromatic interactions in catalyst design see a) Y. Zhao, Y. Domoto, E. Orentas, C. Beuchat, D. Emery, J. Mareda, N. Sakai, S. Matile, *Angew. Chem. Int. Ed.* **2013**, *52*, 9940 – 9943; *Angew. Chem.* **2013**, *125*, 10124 – 10127; b) Y. Zhao, C. Beuchat, Y. Domoto, J. Gajewy, A. Wilson, J. Mareda, N. Sakai, S. Matile, *J. Am. Chem. Soc.* **2014**, *136*, 2101 – 2111; c) Y. Zhao, N. Sakai, S. Matile, *Nat. Commun.* **2014**, *5*, 3911.

[33] For evidence of intramolecular CH–π interactions in pyrolidine organocatalyst derivatives see a) M. B. Schmid, K. Zeitler, R. M. Gschwind, *Chem. Sci.* **2011**, *2*, 1793 – 1803; b) Y. P. Rey, L. E. Zimmer, C. Sparr, E.-M. Tanzer, W. B. Schweizer, H. M. Senn, S. Lakhdar, R. Gilmour, *Eur. J. Org. Chem.* **2014**, 1202 – 1211; c) for a recent study implicating dispersion interaction in organocatalytic Mukaiyama-Michael reactions see E. K. Kemppainen, G. Sahoo, A. Piisola, A. Hamza, B. Kótai, I. Pápai, P. Pihko, *Chem. Eur. J.* **2014**, *20*, 5983 – 5993.

Received: January 21, 2015
Published online on May 15, 2015